Tuning Electronic Properties of Functionalized Polyhedral Oligomeric Silsesquioxanes: A DFT and TDDFT Study

Chang-Gua Zhen,† Udo Becker,‡ and John Kieffer*,†

Department of Materials Science and Engineering and Department of Geological Sciences, University of Michigan, Ann Arbor, Michigan 48109

Received: April 24, 2009; Revised Manuscript Received: June 26, 2009

The structure and electronic properties of polyhedral oligomeric silsesquioxane (POSS) cages functionalized with different organic groups have been studied using density functional theory and time-dependent density functional theory calculations. Accordingly, the POSS-T8 cage is quite rigid upon functionalization and thus provides a means for spatially separating conjugated organic fragments, which is useful for the realization of novel organic molecular architectures for light-emitting diodes. Moreover, electronic properties can be tuned through the choice of functional groups and their positioning on or within the POSS cage. Attaching an electron-donating group, such as 4-carbazolephenyl, to the silicon atom at the corner of the cage raises the HOMO level, while attaching an electron-withdrawing group, such as 4-cyanophenyl, or inserting an inert molecule, such as N_2, into the POSS cage lowers the LUMO level. Frontier orbital analysis indicates that the POSS cage is partially conjugated and serves a role as electron acceptor. Carrier transport rates are discussed in the frame of Marcus' electron hopping theory. On the basis of the calculated reorganization energies, these POSS compounds can be used as carrier transporting or blocking materials, depending on the functionalization. Exciton binding energies strongly depend on the spatial arrangement of frontier orbitals rather than on molecular sizes.

1. Introduction

Today, various types of nanoscale building blocks, such as carbon nanotubes,[1,2] CdS nanowires,[3−6] fullerenes,[7,8] and polyhedral oligomeric silsesquioxanes (POSS) cages,[9,10] can be produced reliably and with high definition. These building blocks serve as the basis for the molecular engineering of new materials and devices with unique properties and functions.[11] Among these designed materials, derivatives of POSS have been widely used as end-cappers[12,13] or pendant units[14,15] to suppress aggregation in conjugated polymers in order to enhance the performance of organic light-emitting diodes (OLEDs). Recently, Sellinger et al. have demonstrated that appropriately functionalized POSS can be directly used in OLEDs as high-efficiency emissive and hole-transport materials.[16,17] However, there are some problems regarding the use of POSS derivatives as semiconductors in organic electronics. Foremost, the energy gaps between highest occupied molecular orbital (HOMO) and lowest unoccupied molecular orbital (LUMO) of POSS and its derivatives are normally too large to allow for semiconductor behavior, because the silica core is not a traditional π-conjugated structure. A possible way to tune the energy level of frontier orbitals is functionalizing the POSS cube with organic groups, thereby creating hybrid organic−inorganic building blocks. The tunability of the energy gap is essential for multicolor electroluminescence and photovoltaic applications. However, the interactions between the silica core and the functional groups and their effect on the electronic structure of the hybrid molecules are not well understood. Therefore, theoretical studies of POSS compounds to clarify how the functional groups affect the optical or electrical properties of these compounds are important in view of guiding the molecular design and synthesis of new nanoscale building blocks for applications in organic electronics.

First-principles studies of POSS systems are computationally intensive because of the size of the molecules in question. As a first endeavor, we therefore investigate the functionalized derivatives of the most commonly used POSS system, i.e., the cube-shaped $H_8Si_8O_{12}$ (POSS-T8). Density functional theory (DFT) and time-dependent density functional theory (TDDFT)[18,19] were utilized to study the ground and excited electronic states of these molecules to obtain an accurate and computationally economical way of modeling electron correlation.[20,21]

2. Molecular Design and Computational Details

In this study, POSS-T8 served as the starting configuration, to which we attached different functional groups in order to tune the frontier orbitals of the POSS compounds, and achieve organic−inorganic nanocomposites with controllable energy gaps, carrier transport properties and exciton binding energies. These functional groups included 4-cyanophenyl (Cy), which generally acts as an electron-withdrawing group, and 4-carbazolephenyl (Car), an electron-donating group. These species were attached to the outside corners of the POSS cube, covalently bonded to silicon, to form Cy-POSS-T8 and Car-POSS-T8 molecules, respectively. Furthermore, we inserted a conjugated system, for instance an N_2 molecule into the center of the POSS cube, to influence the electronic structures of the cage and to probe the chemical environment inside the cube. We examined the electronic structures of hybrid molecules resulting from various combinations of these species, including POSS-T8-N_2, Cy-POSS-T8, Car-POSS-T8, Cy-Car-POSS-T8, and Cy-Car-POSS-T8-N_2, a configuration with the electron-

* To whom correspondence should be addressed. Tel: 734-763-2595. Fax: 734-763-4788. E-mail: kieffer@umich.edu.

† Department of Materials Science and Engineering.

‡ Department of Geological Sciences.

10.1021/jp903796m CCC: $40.75 © 2009 American Chemical Society
Published on Web 08/11/2009

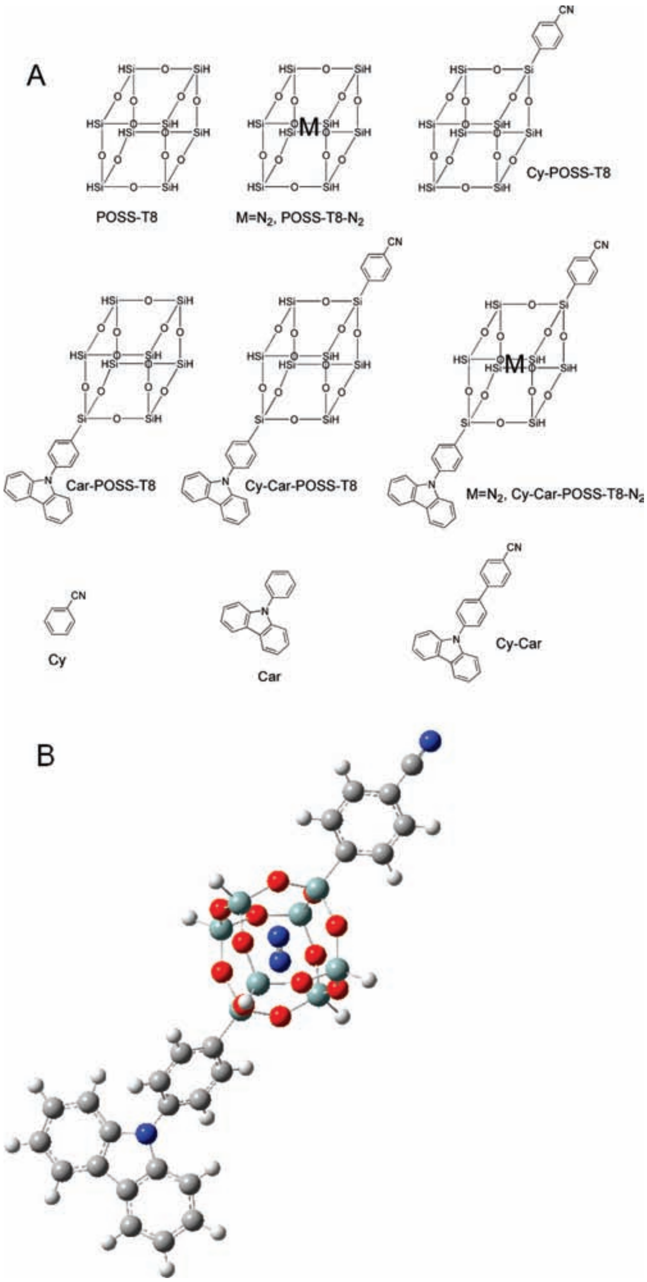

Figure 1. (A) Molecular structures of POSS-T8, its derivatives, and the individual organic functional groups. (B) 3D view of optimized structure of Cy-Car-POSS-T8-N_2. C (black), H (white), O (red), N (blue), Si (gray).

withdrawing and electron-donating groups attached to the silicon atoms on opposite sides of the body diagonal with insertion of N_2 inside the cage. The structures of these molecules are shown in Figure 1(A), in which the organic counterparts without the cage are also included.

Calculations on the above molecules were performed using Gaussian03.[22] Preoptimizations of the molecules were carried out using PM3 semiempirical quantum chemistry model.[23] The resulting molecular configurations were used as the starting atomic coordinates for further optimization in the DFT frame. We chose B3LYP as the exchange-correlation functional.[24] B3LYP is a Hartree−Fock-DFT hybrid where the exchange energy is explicitly calculated using a Hartree−Fock approach. The molecular geometries were optimized in the Cartesian coordinate system without any symmetry (maximum degrees of freedom) using 6-31G* contracted Gaussian basis set with polarization functions.[25,26] The convergence criteria used in the Berny optimization method[27] required the maximum force, rms force, maximum displacement, and rms displacement to be less than 4.5×10^{-4}, 3.0×10^{-4}, 1.8×10^{-3}, 1.2×10^{-3} au, respectively (default values). TDDFT calculations were based on the optimized geometries at the same approximation level, i.e., B3LYP/6-31G*.

3. Results and Discussion

3.1. Ground State Geometries and Frontier Orbitals. POSS-T8 has been widely investigated experimentally and theoretically. Ample experimental data and first-principles calculation results are available to test the reliability of the methodology used in this work. A comparison of the calculation results from this work and other theoretical results and experimental data is presented in Table 1.

The optimized bond lengths and angles are in good agreement with the experimental data and calculation results using other methods. Specifically, the bond length of Si−O and Si−H are a bit longer than the experimental data obtained from X-ray diffraction and neutron diffraction. The reason might be that in our calculations, the molecule is relaxed in vacuum, whereas the experimental data are obtained for the condensed solid state. Differences of bond lengths of Si−O between our calculations and the experimental data are all less than 1.5%. For Si−H bonds, the difference is about 1.0% when compared with neutron diffraction results. For the Si−O−Si bond angle, the difference between the calculations and experiment is less than 1.2%, and those for the O−Si−O or O−Si−H angles are negligibly small.

The silica core is found to be quite rigid, as is revealed by comparing the distance between two silicon atoms along body diagonal before and after functionalization. In POSS-T8, this distance is 5.473 Å. In the hybrid molecules, the spacing between the diagonally opposed silicon atoms, to which an organic group is attached in at least one or both cases, is always larger than that in POSS-T8, but the differences are less than 2.7% (Table 2). The rigidity of the inorganic core in the derivatives is likely to invoke three-dimensional arrangement of these building blocks in an extended structure. This may help to suppress the $\pi-\pi$ stacking between planar conjugated organic fragments attached to the core in solid state, because the organic groups can only assume limited orientations relative to the cube. This unique structural feature may help to prevent the quenching of excitons by intra- and intermolecular interactions, which is a major reason for lowering quantum efficiencies in OLEDs.[12,32−34]

The two nitrogen atoms in POSS-T8-N_2 and Cy-Car-POSS-T8-N_2 are located in the center of the cage, lying on one mirror plane of the cage, and are aligned with the two oxygen atoms in this plane located on the diagonally opposed cube edges (Figure 1(B)). The resulting orientation of nitrogen atoms inside the cage is consistent with a previous high-level ab initio study.[35] The distance between the two nitrogen atoms inside the cage in POSS-T8-N_2 is 1.0954 Å, which is a little shorter than the bond length of 1.1055 Å in an isolated nitrogen molecule, evaluated in the same approximation level. This implies that the two nitrogen atoms are strongly bonded to each other as in the N_2 molecule. The bonded nature of the two nitrogen atoms inside the cage preserves some electronic properties of nitrogen molecule, which will be explained below. In Cy-Car-POSS-T8-N_2, the distance of the two nitrogen atoms inside the cage is 1.0951 Å, almost the same as in POSS-T8-N_2. The difference in bonding energy of the nitrogen atoms in Cy-Car-POSS-T8-N_2 and POSS-T8-N_2 is as small as 4.60×10^{-4} eV, as calculated from B3LYP/6-31G*. To ascertain the minimal effect that

TABLE 1: Selected Geometry Parameters of POSS-T8

methods	bond length(Å) Si−O	Si−H	angle(°) Si−O−Si	O−Si−O	O−Si−H	references
DFT B3LYP/6-31G*	1.643−1.644	1.465	146.1−149.3	109.5−109.8	109.3−109.4	this work
HF 6-31G(d)	1.630	1.457	149.0	109.0		ref 28
DFT B3LYP/6-31G**	1.640	1.460	148.2	109.6	109.3	ref 29
X-ray diffraction	1.619	1.450	147.5	109.6	109.5	ref 30
neutron diffraction	1.623−1.626	1.459−1.463	147.25−147.45	109.14−109.53	109.07−109.77	ref 31

TABLE 2: Distance between the Silicon Atoms on Body Diagonal

	POSS-T8	POSS-T8-N_2	Cy-POSS-T8	Car-POSS-T8	Cy-Car-POSS-T8	Cy-Car-POSS-T8-N_2
distance (Å)	5.473	5.483	5.481	5.492	5.500	5.623
deformation (Å)		0.01	0.008	0.019	0.027	0.15
deformation (%)		0.18	0.15	0.35	0.49	2.7

functionalization of the POSS cage has on its inside chemical environment, we also inserted the more polarizable HF molecule as a probe. In Cy-Car-POSS-T8-HF, the distance of the hydrogen and fluorine atoms inside the cage is 0.9865 Å, while it is 0.9418 Å in POSS-T8-HF. The difference in bonding energy of the hydrogen and fluorine atoms in Cy-Car-POSS-T8-HF and POSS-T8-HF is 6.6×10^{-2} eV. This indicates that the chemical environment inside the cage is not much affected by the functionalization with organic groups outside the cage; it is mainly maintained by the cage itself.

The spatial arrangement of all the frontier orbitals were determined for the ground state optimized geometries corresponding to the singlet spin state for POSS-T8 and its derivatives. The calculated HOMO−LUMO energies of those molecules are shown in Figure 2.

The HOMO energy is −8.47 eV and LUMO energy is 0.38 eV for POSS-T8. The HOMO and LUMO gap is 8.85 eV, which is larger than the value of ∼7.1 eV calculated from DFT using GGA-PW91 exchange and correlation functional with ultrasoft pseudopotentials and a plane-wave basis set, reported by Lin et al. for POSS-T8 arranged in a periodic crystal structure.[36] The HOMO of POSS-T8 originates from the atomic orbitals (AOs) of lone-pair electrons on oxygen atoms, which is also in agreement with the previous reports.[36,37]

By comparing the HOMO and LUMO of POSS-T8 and Cy-POSS-T8, we can see that functionalization of one corner of the cage with the 4-cyanophenyl electron-withdrawing group changes the HOMO energy by about 1 eV, from −8.47 to −7.44 eV, and the LUMO energy more dramatically, from 0.38 to −1.82 eV. The electron density of the LUMO of Cy-POSS-T8 is mainly localized on the 4-cyanophenyl group (Figure 3). For Cy-Car-POSS-T8, the value of the LUMO is similar to that for Cy-POSS-T8, and the principal contribution is also from cyanophenyl group.

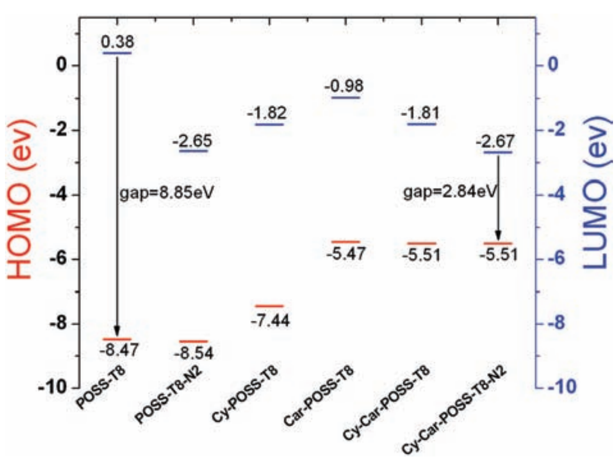

Figure 2. Calculated HOMO and LUMO of POSS-T8 and its derivatives at the approximation level of B3LYP/6-31G*.

However, the HOMO can be effectively tuned by an electron-donating group. The HOMO energies of Car-POSS-T8, Cy-Car-POSS-T8, and Cy-Car-POSS-T8-N_2 are almost the same (∼−5.5 eV). From Figure 3, we can see that all these HOMO are localized in the 4-carbazolephenyl electron-donating group, and share a similar electron density surface.

The HOMO of POSS-T8-N_2 is very similar to that of POSS-T8, i.e., the electron density is mostly localized on the oxygen atoms. But the LUMO of the POSS-T8-N_2 is completely different from that of POSS-T8. In the latter case, the electron density is distributed across all atoms, while the LUMO of POSS-T8-N_2 partially resides on the oxygen atoms, and for the most part on the nitrogen atoms inside the cage. By comparing the frontier orbitals of the nitrogen molecule and POSS-T8-N_2, it is clear that the LUMO of POSS-T8-N_2 mainly consists of the nitrogen π orbital confined to the inside of the cage. As indicated above, the strong covalent bonded between the two nitrogen atoms causes them to preserve the properties of the individual nitrogen molecule instead of a loosely attached atomic cluster. The value of LUMO of POSS-T8-N_2 is 3.03 eV lower than that of POSS-T8, reducing the HOMO−LUMO gap from 8.85 eV for POSS-T8 to 5.89 eV for POSS-T8-N_2.

If the electron-donating and withdrawing groups are both attached to the cage to form Cy-Car-POSS-T8, then the HOMO and LUMO are localized on the two groups respectively and the HOMO−LUMO gap reduces to 3.70 eV, corresponding to the energy of near violet light. Finally, inserting N_2 inside the cage to form Cy-Car-POSS-T8-N_2 does not change the HOMO but changes the LUMO to localize mainly on the nitrogen atoms inside the cage, as in the case of POSS-T8-N_2. The HOMO−LUMO gap is further reduced to 2.84 eV, which falls into the range of visible spectrum.

The silsesquioxane cage is normally considered an insulator. Recently, on the basis of experimental results, Sulaiman et al. suggested that the cage can interact electronically with the conjugation groups attached to the corner.[38] Our calculations directly confirm the above statement by comparing the HOMO and LUMO energy gap of the Cy group taken individually with that of the Cy-POSS-T8 hybrid molecule, or similarly, those of Car and Car-POSS-T8. The HOMO−LUMO gap of Cy-POSS-T8 is lower than that of Cy by 0.19 eV, while the HOMO−LUMO gap of Car-POSS-T8 is, again, lower than that of Car by 0.23 eV. The silica cage in these molecules cannot be simply regarded as a nonconjugated moiety. These organic−inorganic skeletons

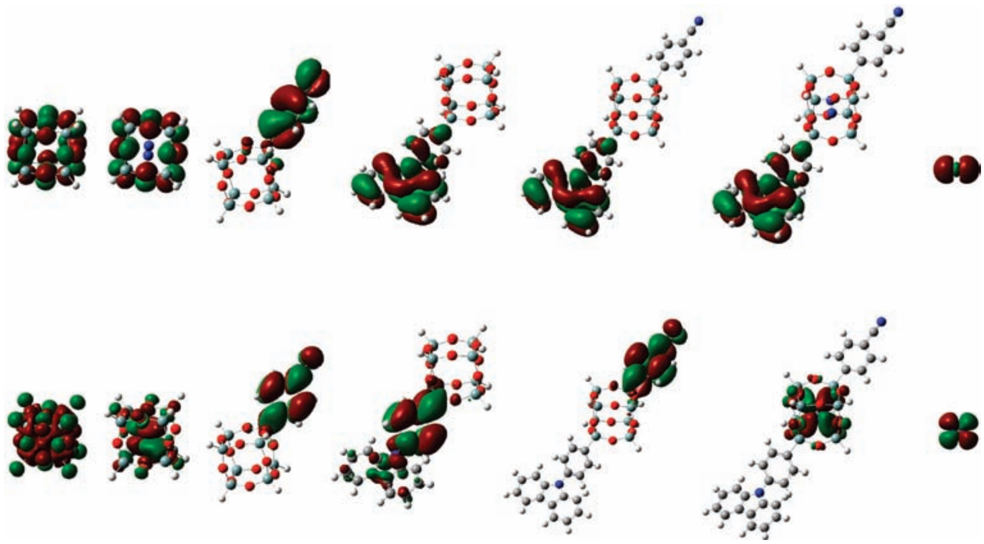

Figure 3. Electron density isocontours (0.02 au). Top: HOMO, bottom: LUMO. From left to right: POSS-T8, POSS-T8-N_2, Cy-POSS-T8, Car-POSS-T8, Cy-Car-POSS-T8, Cy-Car-POSS-T8-N_2, and N_2.

are at least partially conjugated. We also find that the LUMO of Cy-POSS-T8 is lower than that of Cy by 0.41 eV, and the LUMO of Car-POSS-T8 is lower than that of Car by 0.33 eV. The more negative LUMO of POSS derivatives in energy compared with the individual organic semiconductor group by itself reduces the electron injection barrier, indicating that the silica core serves the role as electron acceptor, consistent with the experimental findings by Feher et al.[39]

3.2. Reorganization Energy. Although the unique rigid structures of POSS derivatives may make them good emitters for OLEDs, the organic–inorganic partially conjugated skeleton of these molecules might not perform well with regard to carrier conductivity, which is essential for organic electronics. For organic materials, the conductivity mechanism is normally explained by hopping models. Two main models for the hopping mechanism are often used in the literature, one is expressed by the Miller–Abrahams equation and is valid for weak electron–phonon interactions and at low temperature (far below room temperature);[40] the other one is Marcus' theory, which is applicable in the case of large electron–phonon coupling and at higher temperature.[41] Since organic molecules possess intrinsic intermolecular and intramolecular vibrational modes that are much stronger than usual electron–phonon coupling in inorganic crystals,[42] Marcus' theory is more widely used in organic materials research. On the basis of Marcus theory, the conductivity of amorphous organic materials depends on the electron (or hole) transfer reactions between two adjacent molecules (hopping sites), represented by M_1 and M_2

$$M_1^{+/-} + M_2 \rightarrow M_1 + M_2^{+/-} \tag{1}$$

for which the hopping rate can be described by Marcus' electron transfer equation:

$$k_{et} = \frac{2\pi}{\hbar}\frac{H_{da}^2}{\sqrt{4\pi\lambda kT}}\exp\left(-\frac{(\Delta G + \lambda)^2}{4\lambda kT}\right) \tag{2}$$

where λ is the reorganization energy, H_{da} is the charge-transfer integral, ΔG is the free energy change for the electron transfer reaction, and T is temperature. In the case that the hopping

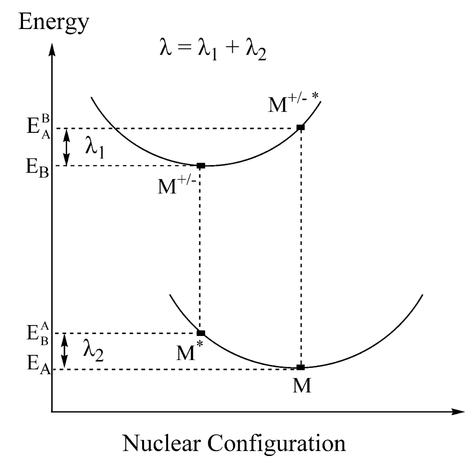

Figure 4. Schematic illustration of the configuration adjustment during self-exchange charge transfer reaction and the calculation of the internal reorganization energy.

process occurs between identical molecules, ΔG is zero. The charge transfer integral, H_{da}, is determined by the overlap of wave function between adjacent molecules, which is determined by the relative spatial overlap and patterns of the wave function.[43] In amorphous organic semiconductors, molecular packing is random. As a result, the hopping rate in the path of carriers samples a distribution of intermolecular distances and orbital overlaps and will likely converge toward similar values within a few hops for molecules that possess similar structures and electron density. Therefore, within a particular family of molecules, H_{da} can be expected to constitute a less variable quantity than the reorganization energy, which represents the activation barrier originated from the configuration adjustment of molecules during the charge transfer. The reorganization energy λ consists of inner reorganization energy and external polarization due to the solvent effects of the surrounding medium. The latter contribution is less important in solid state, which is supported by recent theoretical results on charge transfer in organic materials using inner reorganization energy.[44,45] The reorganization energies are obtained by comparing the energies in the charged and uncharged optimized configurations, for both the neutral and ionized states, as illustrated in Figure 4. Accordingly, $\lambda = E_A^B - E_B + E_B^A - E_A$, where E_A^B is the energy of the ion in the optimized uncharged geometry, E_B is the energy

TABLE 3: Reorganization Energies of POSS Derivatives[a]

	Cy-POSS-T8	Cy	Car-POSS-T8	Car	Cy-Car-POSS-T8	Cy-Car	Cy-Car-POSS-T8-N_2
λ_- (eV)	0.939 (0.879)	0.383 (0.363)	0.829 (0.756)	0.370 (0.256)	0.454 (0.441)	0.515 (0.499)	3.16 (3.04)
λ_+ (eV)	0.612 (0.621)	0.255 (0.253)	0.206 (0.204)	0.098 (0.100)	0.208 (0.210)	0.102 (0.104)	0.245 (0.229)

[a] Data not in parentheses are obtained from single point energy calculations using 6-31G* based on geometries optimized in 6-31G*. Data in parentheses are obtained from single point energy calculations using 6-31+G* based on geometries optimized in 6-31G*.

TABLE 4: Exciton Binding Energy (E_b) of POSS Derivatives

	POSS-T8	POSS-T8-N_2	Cy-POSS-T8	Cy	Car-POSS-T8	Car	Cy-Car-POSS-T8	Cy-Car	Cy-Car-POSS-T8-N_2
E_b (eV)	0.987	1.01	0.611	0.678	0.618	0.643	0.181	0.426	0.305

of the ion in the optimized charged geometry, E_B^A is the energy of the neutral molecule in the optimized charged geometry, and E_A is the energy of the neutral molecule in the optimized uncharged geometry.

To select suitable basis sets for calculating reorganization energies, we carried out exploratory calculations on Cy and Cy-POSS-T8 using various basis sets, and benchmarked the results against those obtained with a very large basis sets such as 6-311++G(3df,3pd) for both geometry optimizations and single point energy calculations. (see Supporting Information Figures S1 and S2). Accordingly, calculations using the 6-31G* basis set for both the geometry optimization and the single point energy calculations yield reorganization energies that deviate from these reference values by no more than 0.021 eV for Cy and 0.081 eV for Cy-POSS-T8, which is acceptable judged against the spread in the data reported in the current literature. Using the 6-31+G* basis set for single point energy calculations on geometries optimized in the 6-31G* set, reduces the deviations to less than 0.012 eV for Cy and less than 0.048 eV for Cy-POSS-T8. This improvement that may be justified weighed against the additional computational cost, since it does not affect the trend in our data. The calculated reorganization energies for electron transfer (λ_-) and for hole transfer (λ_+) are listed in Table 3 for both calculation approaches.

The data in Table 3 suggest the following trends. First, the λ_- values are larger than λ_+ for all compounds. If we only consider the activation energies for carrier hopping and neglect the charge transfer integral, then these compounds are expected to be better hole than electron transporters. For compounds with the carbazole moiety, this is consistent with the well-known fact that this molecular group is a good hole transporter. But it is surprising that even for Cy and Cy-POSS-T8, λ_- values are larger than λ_+, because they are supposed to be an electron transporter due to the electron-withdrawing characteristic of the cyanophenyl group. Second, the reorganization energies of the functionalized POSS compounds are generally larger than the corresponding organic groups by themselves, except that λ_- for Cy-Car-POSS-T8 is slightly smaller than that of Cy-Car. This general trend suggests that the energy associated with the silica cage reconfiguration in these molecules during the carrier hopping process may be quite large. On the basis of comparing reorganization energies, these organic−inorganic hybrid composites are not good carrier transporters compared to the organic groups alone, assuming that the difference of the charge transfer integral is negligible.

We are particularly interested in the charge transport properties of Cy-Car-POSS-T8-N_2 because of its tremendously large λ_-. Since the HOMO of neutral Cy-Car-POSS-T8-N_2 is mainly localized on the π orbitals of the nitrogen atoms inside the cage, electrons entering this molecule will prefer to be localized around the nitrogen atoms. This will induce reconfiguration of the nitrogen atoms and the rigid cage around them (see Supporting Information). Indeed, the distance between the two nitrogen atoms changes from 1.0951 Å to 1.1609 Å. The difference in bonding energy of the nitrogen atoms in the neutral and negatively charged molecules is 0.20 eV, as calculated using B3LYP/6-31G*. In contrast, the distance between the two nitrogen atoms inside the cage in a positively charged molecule is 1.0950 Å, nearly identical to the value for neutral Cy-Car-POSS-T8-N_2, where it is 1.0951 Å.

On the basis of eq 2, if we disregard the difference in charge transfer integrals for electron and hole transport, then the relative hopping rate of holes versus electrons of Cy-Car-POSS-T8-N_2 is about $10^{12}\sim10^{13}$. In fact, the LUMO of Cy-Car-POSS-T8-N_2 is mostly located inside the cage, which hinders the wave function overlap of the LUMOs of neighboring molecules. This leads to a small charge transfer integral for electron transport compared to that for hole transport. The hole/electron hopping rate ratio is expected to be even larger if charge transfer integrals are considered. On the basis of our predictions, Cy-Car-POSS-T8-N_2 might be used as electron-blocking materials due to the large electron transfer barrier. Electron and hole blocking materials are widely used in organic light-emitting diodes to enhance the quantum efficiencies.[46−48] Normally, materials with deep HOMO (high ionization potential) can be used as a hole-blocking layer, while materials with high-lying LUMO (low electron affinity) can be used as an electron blocking layer.[49] For these materials, the blocking effects are due to high charge injection barriers. Conversely, Cy-Car-POSS-T8-N_2 would possibly be a compound whose electron blocking effect was due to charge transport barriers rather than charge injection barrier.

3.3. Exciton Binding Energy. The exciton binding energy (E_b) is another important quantity that determines the optoelectronic properties in organic materials and devices.[50] It is directly related to the charge separation in organic solar cells and hence, it is an important factor for the efficiency of the cells.[51] It also affects the quantum efficiency of OLEDs[52] because the emissive singlet fraction of excitons in organic light-emitting diodes depends on the exciton binding energy.[53,54] Normally, the intermolecular interactions in amorphous organic solids are not as strong as that in inorganic crystalline semiconductors, so that the exciton is Frenkel type (the exciton is localized in a single molecule) in organic materials, while is Wannier−Mott type in inorganic materials.[55] Recent time-resolved spectroscopy investigation revealed that the primary exciton generated from polycrystalline pentacene is Frenkel type, before this excited state delocalizes to excimers.[56] Hence, calculation from gas phase molecules results in a reasonable approximation for E_b of organic amorphous materials.

An exciton can be modeled as a two-electron system: one electron is excited into a higher-energy orbital while leaving a hole in a partially filled lower-energy orbital.[57] Since the exciton binding energy mainly originates from the Coulomb interactions between the electron and hole,[50] the spatial distribution of the

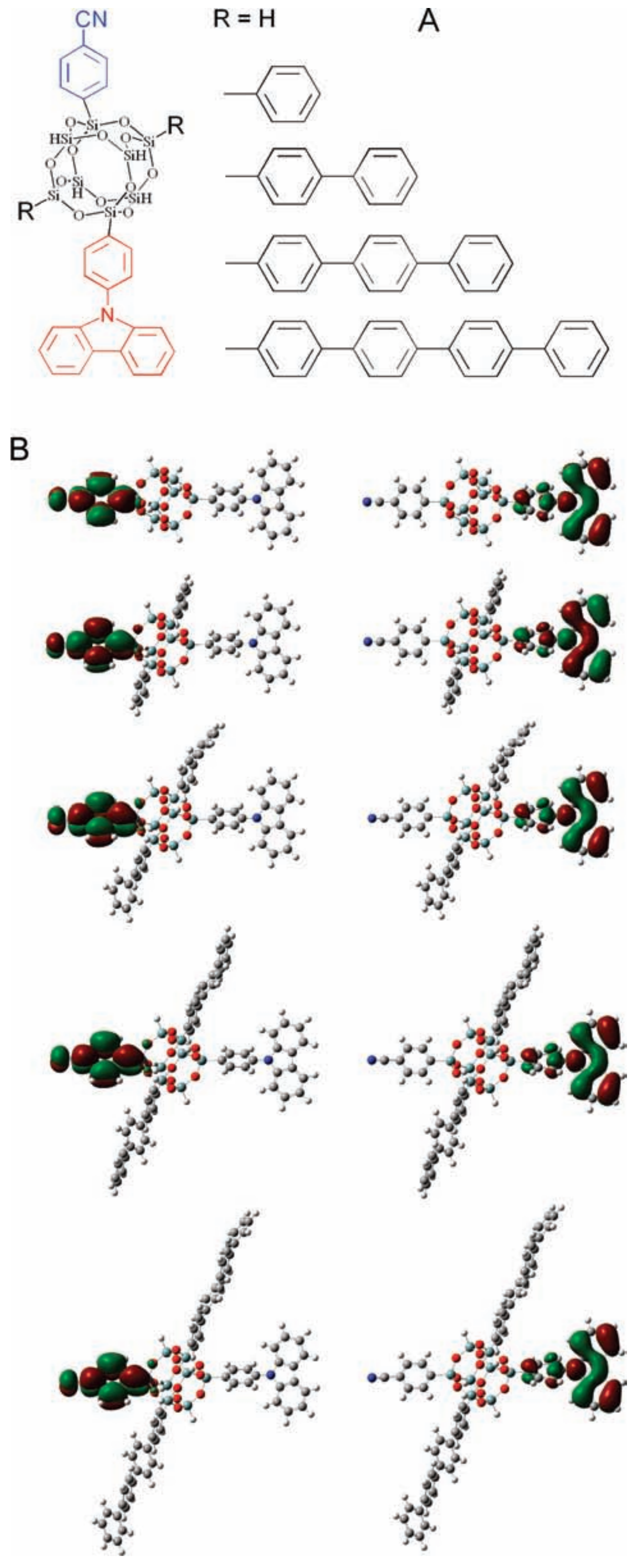

Figure 5. (A) Molecular structures of POSS derivatives with fixed electron-donating group and electro-withdrawing group attached to the POSS cage while increasing the length of the side groups. Exciton binding energies for these molecules are all equal to 0.181 eV. (B) Electron iso-density contours (0.02 au), left: LUMO, right: HOMO.

density of electrons in the LUMO and that of holes in HOMO should be decisive. Therefore, a simple way to lower the exciton binding energy is to separate LUMO and HOMO in space as far as possible. In organic molecules, the HOMO is mainly localized in electron-donating groups and the LUMO in electron-withdrawing groups, as indicated in section **3.1**. On the basis

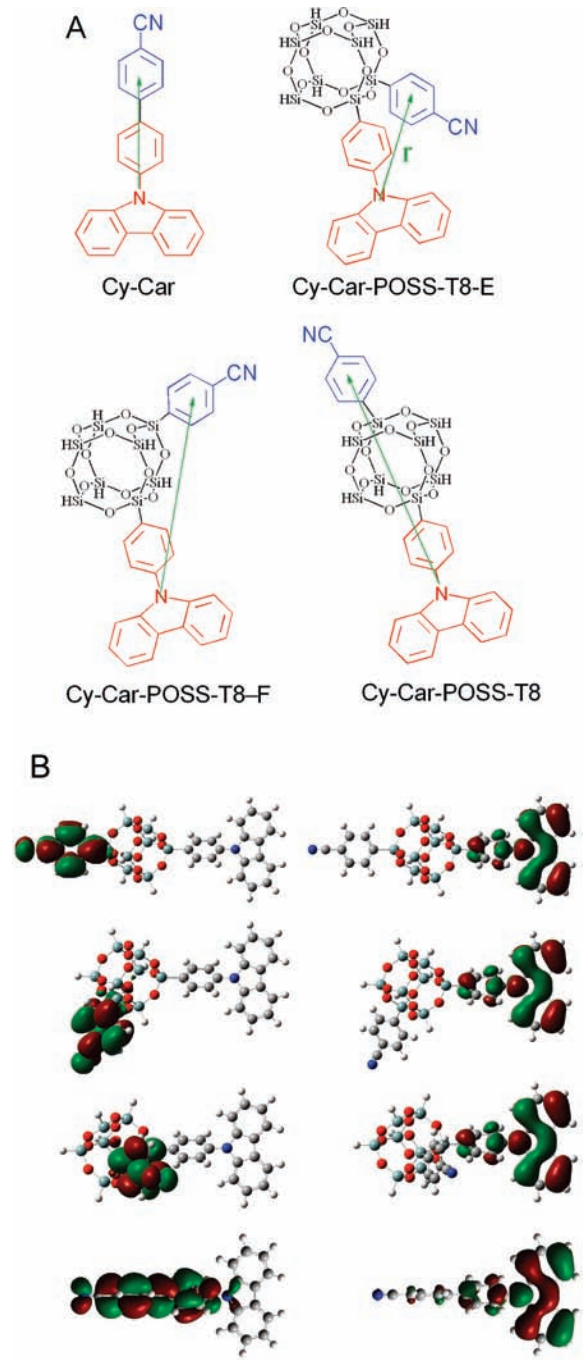

Figure 6. (A) Molecular structures of POSS derivatives with electron-donating group and electron-withdrawing group attached to the POSS cage in different positions. The green arrows indicate the spatial separation between HOMO and LUMO. (B) Electron iso-density contours (0.02 au), left: LUMO, right: HOMO.

of the above analysis, the exciton binding energy of Cy-Car-POSS-T8 is expected to be the lowest in the POSS derivatives, given that the HOMO and LUMO are well separated (Figure 3).

Experimentally determined exciton binding energies for organic semiconductors normally range from 0.1 to 1.5 eV, and even vary for the same compound due to variations in experimental conditions reported by different research groups. The estimation of E_b from theory can also be done using different approaches, which has been discussed before.[58] Here, we will start from the common description of the exciton binding energy in which E_b can be taken as the difference between the

TABLE 5: Exciton Binding Energy (E_b) of POSS Derivatives with the Functional Groups Attached at Various Positions in POSS Cage

	Cy-Car-POSS-T8	Cy-Car-POSS-T8-F	Cy-Car-POSS-T8-E	Cy-Car
E_b (eV)	0.181	0.218	0.294	0.426

electronic and optical bandgap energies.[59] For small molecules with localized wave functions, the electronic bandgap is approximated as energy difference of HOMO and LUMO, while the optical gap is taken as first excitation energy.[58] The calculations of the excitation energy are performed using TDDFT at the same level as was used for the molecular structure optimizations. The calculated exciton binding energies of the POSS and POSS derivatives are listed in Table 4.

The calculated exciton binding energy for Cy-Car-POSS-T8 is much smaller than that for Cy-Car, because the POSS core separates the electron-donating group and the electron-withdrawing group, where the HOMO and LUMO are localized. We also notice that E_b of Cy-Car-POSS-T8-N_2 is larger than Cy-Car-POSS-T8. A possible reason is that the LUMO for Cy-Car-POSS-T8-N_2 is localized on the nitrogen atoms inside the POSS cage rather than in the cyanophenyl group. Thus, the distance between the HOMO and LUMO orbitals is shortened. It seems that E_b depends on the spatial distribution of HOMO and LUMO rather than on molecular size, since the two molecules in this case have the same spatial extents. To solidify this speculation, we further compared E_b for molecules (I) with different sizes in dimensions but similar HOMO and LUMO distributions, and (II) with similar size but different HOMO and LUMO distributions.

For (I), we design the molecules with the cyanophenyl and carbazolephenyl groups attached to the opposite corners of the POSS cube along the body-diagonal, i.e., at a fixed distance, while attaching polyphenyl moieties with different lengths to another pair of diagonally opposed corners of the POSS cube (Figure 5). The number of benzene rings in the polyphenyl moieties is varied from 0 to 4. Accordingly, the molecule lengths range from 5.7 to 43 Å, measured along the polyphenyl moieties. The distribution of the HOMO and LUMO are similar for all these molecules, i.e., the HOMO is mainly localized in carbazolephenyl group and the LUMO in cyanophenyl group. Our calculated E_b for all these molecules are identical to that of Cy-Car-POSS-T8, which is consistent with our conjecture.

For (II), we attached the cyanophenyl group and carbazole-phenyl groups to different silicon atoms along body-diagonal (Cy-Car-POSS-T8), face-diagonal (Cy-Car-POSS-T8-F), or the same edge of the cube (Cy-Car-POSS-T8-E), so that the distance between the electron donating and withdrawing functional groups varies (Figure 6). For this series of molecules, we found that E_b is closely correlated with the spacing between those two types of organic functional groups in the molecule (Table 5).

Further analysis shows that E_b is proportional to the reciprocal of the distance between electron donating and withdrawing groups, where this distance was measured from the nitrogen atom in the carbazole group to the center of the benzene ring in the cyanophenyl group (Figure 7), which represent the spatial separation of HUMO and LUMO. This proportionality originates from the fact that the HOMO and LUMO mainly occupy a small space in carbazolephenyl and cyanophenyl groups and are well separated so that the interaction between the electron in LUMO and the hole in HOMO can be estimated as the electrostatic potential energy between two point-like particles,

$$U_E = \frac{1}{4\pi\varepsilon_0\varepsilon_r}\frac{q_1q_2}{r} \tag{3}$$

where ε_0 is electric constant, ε_r is dielectric constant, q_1 and q_2 are the charge of two particles, and r is the distance between the two particles. For diffusive or severely overlapping HOMO and LUMO (as in the case of Cy-POSS-T8 or Car-POSS-T8), the proportionality between E_b and r does not hold because the point-like approximation is no longer accurate. In these cases, the interaction of electron and hole in HOMO and LUMO does not simply depend on the molecule length any more, nor does the exciton binding energy.

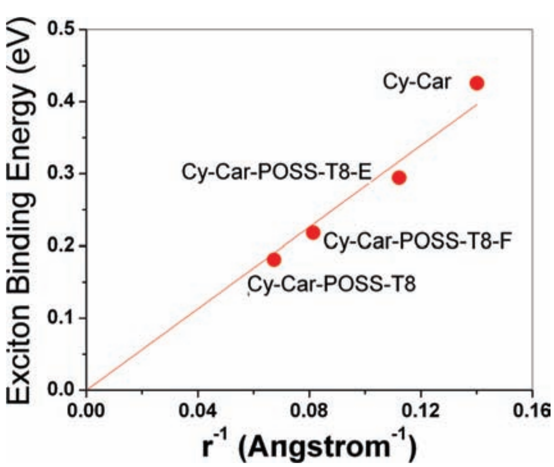

Figure 7. Correlation between the exciton binding energies and the spatial separation of HOMO and LUMO. The red line is a linear fit.

4. Conclusions

On the basis of studying the structure and electronic properties of POSS-T8 and its functionalized derivatives using DFT and TDDFT calculations, we can report the following findings:

(1) The inorganic core of the POSS-T8 is quite rigid. The deformation of the POSS core upon functionalizing the corners of the cube with organic groups and/or by inserting an N_2 molecule inside the cage is very small. The rigidity of the POSS cube may help to prevent the aggregation of planar organic conjugated fragments, which is important in some organic electronics devices such as OLEDs. The POSS derivatives therefore constitute candidates for highly efficient emitters in OLEDs.

(2) The POSS cage is partially conjugated and serves a role as electron acceptor. The energy gap of POSS-T8 can be tuned through functionalization. The HOMO and LUMO can be independently controlled by attaching organic functional groups or inserted inorganic atomic clusters, which provides the flexibility to design molecules with targeted properties and for specific applications. The energy range within which the HOMO−LUMO gap can be tuned includes that of visible light, indicating a potential application of POSS compounds for OLEDs and organic solar cells.

(3) The reorganization energies of POSS derivatives are generally larger than those of the organic functional groups taken by themselves, implying that the hybrid organic−inorganic molecules exhibit poorer carrier transport properties than their organic counterparts. Unlike commonly used carrier blocking materials due to a carrier injection barrier, Cy-Car-POSS-T8-N_2 may be used as electron blocking material due to its large electron transport barrier.

(4) The exciton binding energy for Cy-Car-POSS-T8 is quite small compared with Cy-Car because the POSS cage separates the electron-donating and electron-withdrawing groups where the HOMO and LUMO are localized. Further study of the correlation between the exciton binding energy and molecular structures indicates that E_b is closely related to the spatial separation between HOMO and LUMO.

Although this investigation focuses on a specific POSS system, the calculation results on the designed molecular structures are expected to be applicable in a broader context for organic molecular materials and organic−inorganic hybrid structures that are useful for organic electronics.

Acknowledgment. C.-G.Z. acknowledges support through an MMPEI-Rackham Energy Fellowship at the University of Michigan.

Supporting Information Available: Reorganization energies of Cy and Cy-POSS-T8 calculated using different basis sets and bond length changes between optimized neutral and charged geometries. This material is available free of charge via the Internet at http://pubs.acs.org.

References and Notes

(1) Ebbesen, T. W.; Ajayan, P. M. *Nature* **1992**, *358*, 220–222.
(2) Jarillo-Herrero, P.; van Dam, J. A.; Kouwenhoven, L. P. *Nature* **2006**, *439*, 953–956.
(3) Routkevitch, D.; Bigioni, T.; Moskovits, M.; Xu, J. M. *J. Phys. Chem.* **1996**, *100*, 14037–14047.
(4) Zhan, J. H.; Yang, X. G.; Wang, D. W.; Li, S. D.; Xie, Y.; Xia, Y.; Qian, Y. T. *Adv. Mater.* **2000**, *12*, 1348–1351.
(5) Barrelet, C. J.; Wu, Y.; Bell, D. C.; Lieber, C. M. *J. Am. Chem. Soc.* **2003**, *125*, 11498–11499.
(6) Liang, Y. Q.; Zhen, C. G.; Zou, D. C.; Xu, D. S. *J. Am. Chem. Soc.* **2004**, *126*, 16338–16339.
(7) Adams, G. B.; Sankey, O. F.; Page, J. B.; Okeeffe, M.; Drabold, D. A. *Science* **1992**, *256*, 1792–1795.
(8) Scott, L. T.; Boorum, M. M.; McMahon, B. J.; Hagen, S.; Mack, J.; Blank, J.; Wegner, H.; de Meijere, A. *Science* **2002**, *295*, 1500–1503.
(9) Lichtenhan, J. D. *Comments Inorg. Chem.* **1995**, *17*, 115–130.
(10) Sellinger, A.; Laine, R. M. *Chem. Mater.* **1996**, *8*, 1592–1593.
(11) Lamm, M. H.; Chen, T.; Glotzer, S. C. *Nano Lett.* **2003**, *3*, 989–994.
(12) Xiao, S.; Nguyen, M.; Gong, X.; Cao, Y.; Wu, H. B.; Moses, D.; Heeger, A. J. *Adv. Funct. Mater.* **2003**, *13*, 25–29.
(13) Fenenko, L.; Nakanishi, Y.; Tokito, S.; Konno, A. *Jpn. J. Appl. Phys., Part 1* **2006**, *45*, 550–554.
(14) Lee, J.; Cho, H. J.; Jung, B. J.; Cho, N. S.; Shim, H. K. *Macromolecules* **2004**, *37*, 8523–8529.
(15) Chou, C. H.; Hsu, S. L.; Dinakaran, K.; Chiu, M. Y.; Wei, K. H. *Macromolecules* **2005**, *38*, 745–751.
(16) Lo, M. Y.; Zhen, C. G.; Lauters, M.; Jabbour, G. E.; Sellinger, A. *J. Am. Chem. Soc.* **2007**, *129*, 5808–5809.
(17) Sellinger, A.; Tamaki, R.; Laine, R. M.; Ueno, K.; Tanabe, H.; Williams, E.; Jabbour, G. E. *Chem. Comm.* **2005**, 3700–3702.
(18) Runge, E.; Gross, E. K. U. *Phys. Rev. Lett.* **1984**, *52*, 997–1000.
(19) Jamorski, C.; Casida, M. E.; Salahub, D. R. *J. Chem. Phys.* **1996**, *104*, 5134–5147.
(20) Amekraz, B.; Tortajada, J.; Morizur, J. P.; Gonzalez, A. I.; Mo, O.; Yanez, M.; Leito, I.; Maria, P. C.; Gal, J. F. *New J. Chem.* **1996**, *20*, 1011–1021.
(21) Goldstein, E.; Beno, B.; Houk, K. N. *J. Am. Chem. Soc.* **1996**, *118*, 6036–6043.
(22) Frisch, M. J.; Trucks, G. W.; Schlegel, H. B.; Scuseria, G. E.; Robb, M. A.; Cheeseman, J. R.; Montgomery, J. A., Jr.; Vreven, T.; Kudin, K. N.; Burant, J. C.; Millam, J. M.; Iyengar, S. S.; Tomasi, J.; Barone, V.; Mennucci, B.; Cossi, M.; Scalmani, G.; Rega, N.; Petersson, G. A.; Nakatsuji, H.; Hada, M.; Ehara, M.; Toyota, K.; Fukuda, R.; Hasegawa, J.; Ishida, M.; Nakajima, T.; Honda, Y.; Kitao, O.; Nakai, H.; Klene, M.; Li, X.; Knox, J. E.; Hratchian, H. P.; Cross, J. B.; Bakken, V.; Adamo, C.; Jaramillo, J.; Gomperts, R.; Stratmann, R. E.; Yazyev, O.; Austin, A. J.; Cammi, R.; Pomelli, C.; Ochterski, J. W.; Ayala, P. Y.; Morokuma, K.; Voth, G. A.; Salvador, P.; Dannenberg, J. J.; Zakrzewski, V. G.; Dapprich, S.; Daniels, A. D.; Strain, M. C.; Farkas, O.; Malick, D. K.; Rabuck, A. D.; Raghavachari, K.; Foresman, J. B.; Ortiz, J. V.; Cui, Q.; Baboul, A. G.; Clifford, S.; Cioslowski, J.; Stefanov, B. B.; Liu, G.; Liashenko, A.; Piskorz, P.; Komaromi, I.; Martin, R. L.; Fox, D. J.; Keith, T.; Al-Laham, M. A.; Peng, C. Y.; Nanayakkara, A.; Challacombe, M.; Gill, P. M. W.; Johnson, B.; Chen, W.; Wong, M. W.; Gonzalez, C.; Pople, J. A. Gaussian 03, revision C.02; Gaussian, Inc.: Wallingford, CT, 2004.
(23) Stewart, J. J. P. *J. Comput. Chem.* **1989**, *10*, 209–220.
(24) Becke, A. D. *J. Chem. Phys.* **1993**, *98*, 5648–5652.
(25) Hehre, W. J.; Ditchfie, R.; Pople, J. A. *J. Chem. Phys.* **1972**, *56*, 2257–2261.
(26) Francl, M. M.; Pietro, W. J.; Hehre, W. J.; Binkley, J. S.; Gordon, M. S.; Defrees, D. J.; Pople, J. A. *J. Chem. Phys.* **1982**, *77*, 3654–3665.
(27) Schlegel, H. B. *J. Comput. Chem.* **1982**, *3*, 214–218.
(28) Earley, C. W. *J. Phys. Chem.* **1994**, *98*, 8693–8698.
(29) Mattori, M.; Mogi, K.; Sakai, Y.; Isobe, T. *J. Phys. Chem. A* **2000**, *104*, 10868–10872.
(30) Larsson, K. *Ark. Kemi.* **1960**, *16*, 215–219.
(31) Tornroos, K. W. *Acta Crystallogr., Sect. C* **1994**, *50*, 1646–1648.
(32) Wu, W. C.; Yeh, H. C.; Chan, L. H.; Chen, C. T. *Adv. Mater.* **2002**, *14*, 1072.
(33) Huang, C.; Zhen, C. G.; Su, S. P.; Loh, K. P.; Chen, Z. K. *Org. Lett.* **2005**, *7*, 391–394.
(34) Aubouy, L.; Gerbier, P.; Guerin, C.; Huby, N.; Hirsch, L.; Vignau, L. *Synth. Met.* **2007**, *157*, 91–97.
(35) Tejerina, B.; Gordon, M. S. *J. Phys. Chem. B* **2002**, *106*, 11764–11770.
(36) Lin, T. T.; He, C. B.; Xiao, Y. *J. Phys. Chem. B* **2003**, *107*, 13788–13792.
(37) Calzaferri, G.; Hoffmann, R. *J. Chem. Soc., Dalton Trans.* **1991**, 917–928.
(38) Sulaiman, S.; Bhaskar, A.; Zhang, J.; Guda, R.; Goodson, T.; Laine, R. M. *Chem. Mater.* **2008**, *20*, 5563–5573.
(39) Feher, F. J.; Budzichowski, T. A. *J. Organomet. Chem.* **1989**, *379*, 33–40.
(40) Miller, A.; Abrahams, E. *Phys. Rev.* **1960**, *120*, 745–755.
(41) Marcus, R. A.; Sutin, N. *Biochim. Biophys. Acta* **1985**, *811*, 265–322.
(42) Coropceanu, V.; Cornil, J.; da Silva, D. A.; Olivier, Y.; Silbey, R.; Bredas, J. L. *Chem. Rev.* **2007**, *107*, 926–952.
(43) Bredas, J. L.; Calbert, J. P.; da Silva, D. A.; Cornil, J. *Proc. Natl. Acad. Sci. U.S.A.* **2002**, *99*, 5804–5809.
(44) Yang, X. D.; Wang, L. J.; Wang, C. L.; Long, W.; Shuai, Z. G. *Chem. Mater.* **2008**, *20*, 3205–3211.
(45) Hutchison, G. R.; Ratner, M. A.; Marks, T. J. *J. Am. Chem. Soc.* **2005**, *127*, 16866–16881.
(46) Tsutsui, T.; Aminaka, E.; Tokuhisa, H. *Synth. Met.* **1997**, *85*, 1201–1204.
(47) Mitschke, U.; Bauerle, P. *J. Mater. Chem.* **2000**, *10*, 1471–1507.
(48) Kulkarni, A. P.; Tonzola, C. J.; Babel, A.; Jenekhe, S. A. *Chem. Mater.* **2004**, *16*, 4556–4573.
(49) Adamovich, V. I.; Cordero, S. R.; Djurovich, P. I.; Tamayo, A.; Thompson, M. E.; D'Andrade, B. W.; Forrest, S. R. *Org. Electron.* **2003**, *4*, 77–87.
(50) Franceschetti, A.; Zunger, A. *Phys. Rev. Lett.* **1997**, *78*, 915–918.
(51) Gregg, B. A. *J. Phys. Chem. B* **2003**, *107*, 4688–4698.
(52) Cao, Y.; Parker, I. D.; Yu, G.; Zhang, C.; Heeger, A. J. *Nature* **1999**, *397*, 414–417.
(53) Karabunarliev, S.; Bittner, E. R. *Phys. Rev. Lett.* **2003**, *90*, 057402.
(54) Chen, L. P.; Zhu, L. Y.; Shuai, Z. G. *J. Phys. Chem. A* **2006**, *110*, 13349–13354.
(55) Roslyak, O.; Birman, J. L. *Phys. Rev. B* **2007**, *75*, 245309.
(56) Marciniak, H.; Fiebig, M.; Huth, M.; Schiefer, S.; Nickel, B.; Selmaier, F.; Lochbrunner, S. *Phys. Rev. Lett.* **2007**, *99*, 176402.
(57) Baldo, M.; Segal, M. *Phys. Status Solidi A* **2004**, *201*, 1205–1214.
(58) Sun, M. T.; Kjellberg, P.; Beenken, W. J. D.; Pullerits, T. *Chem. Phys.* **2006**, *327*, 474–484.
(59) Scholes, G. D.; Rumbles, G. *Nat. Mater.* **2006**, *5*, 683–696.

JP903796M